International Journal of Engineering Trends and Technology
ISSN: 2231–5381 / https://doi.org/10.14445/22315381/IJETT-V73I11P121
Volume 73 Issue 11, 295-311, November 2025

Original Article

Elastic Stability of Steel Frames Considering Joints' Rigidity

Hazem Kassab[1], Ezzeldin Sayed-Ahmed[2], Emam Soliman[3]

[1,3]*Department of Structural Engineering, Ain Shams University, Cairo, Egypt.*
[2]*Department of Construction Engineering, The American University in Cairo, Egypt.*

[1]*Corresponding Author : 2201011@eng.asu.edu.eg*

Received: 06 August 2025 Revised: 12 November 2025 Accepted: 15 November 2025 Published: 25 November 2025

Abstract *- This research addresses the effect of joint flexibility on the elastic stability of steel frames. A mathematical framework utilizing the classical stability functions is proposed to derive the governing critical load equations of flexibly jointed frame structures. Through these equations, it is revealed that the critical load is controlled not by the absolute stiffness of beams, columns, or joints but by their relative stiffness ratios. The framework is demonstrated by analyzing a theoretical case study of a single-storey rectangular frame with semi-rigid joints in two scenarios: sway-permitted and sway-prevented (i.e., braced). The analysis indicates variations up to 77% in buckling capacity for frames having connections classified as semi-rigid according to current codes of practice. To verify theoretical predictions, a custom-built software program, "stableX," is introduced. This stiffness-method-based program is designed to accommodate flexible joints and is used in this paper to perform eigenvalue buckling analysis on the single-storey semi-rigid frame. The program not only accurately verifies the analytical results but also serves as a practical, versatile, and efficient numerical method of analysis when more complicated geometries, loading conditions, or boundary constraints are present. The numerical procedures underlying the implementation of "stableX" are detailed in this paper.*

Keywords *- Buckling of Frames, Elastic Stability, Joint Flexibility, Stability Functions, Semi-rigid Connections.*

1. Introduction

The subject of stability is concerned with the study of the equilibrium of structures in their deformed state under sustained compressive forces. Under such conditions, structures experience additional straining actions that regular first-order analysis cannot foresee. In the 16th century, Euler was the first to examine the stability of a pinned-pinned column. He derived a formula to predict its critical buckling load, which, if exceeded, the column is deemed to be in unstable equilibrium. [1] At the critical load and beyond, any perturbation to the column causes very large lateral displacements. In theory, it is said that the column has two equilibrium states at the critical load: the fundamental equilibrium state, where the column remains straight, and the bifurcated equilibrium state, where the column displaces laterally. [2] In real life, columns are never perfectly straight, loads are rarely concentric, and material is never perfectly homogenous. These, among other assumptions made in the theory, make the first equilibrium state impossible to sustain. Real structures typically experience very large lateral displacements (i.e., instability) that often lead to collapse when the load approaches the critical load. Euler's findings laid the foundation for subsequent advancements in stability analysis of structures. The 20th century witnessed significant progress on the subject. For example, the works of Timoshenko are a landmark contribution to the field. [3] This comprehensive work included the study of the stability of a wide range of structural elements such as beam-columns, frames, and plates. Moreover, Timoshenko extended the analysis to other modes of buckling, such as torsional and lateral torsional buckling, and provided an approach to stability analysis using energy methods. Reference [4] is another notable work in the same era that introduced a formal and systematic approach to framework stability. Later, the English school adopted a more systemised approach through stability functions, following in the steps of the slope deflection method. [5] In the stability functions method, fixed end moments for each beam and column in the structure are formulated and then assembled through equilibrium equations at each joint in the structure. These equations are then solved simultaneously to obtain the buckling load. Stability functions were derived for various loading and boundary conditions for frame elements and were made readily available for use. [6] As digital computing emerged in the mid-20th century, scientists in the aeronautical and aerospace industries contemporarily developed matrix methods of analysis that are systematic enough to be programmed as a set of instructions and fed into the computer. [7,8] Their efforts arose from the

need to find faster and more efficient methods of analysis that can deal with the complexity and variability of air and space vehicles' structures. These efforts led to the development of the stiffness method and the first coining of the term "finite-element method", which marked a significant leap in the field of structural mechanics and the rise of a new field, computational structural mechanics. The rapid progress that followed on these numerical methods enabled the development of incremental nonlinear analysis techniques that accommodated both geometrical and material nonlinearities; these are often called second-order analyses. [8-11] Geometrical nonlinearities are necessary in studying the stability of all types of structures. As their name suggests, they depend on the geometry and slenderness of the elements and are not related to the yielding or ultimate strength of the material; however, they depend on the material's modulus of elasticity. Material nonlinearities, on the other hand, are concerned with stress-strain characteristics of the material from the onset of loading up to fracture. [12]

Nowadays, computational methods of analysis, such as the stiffness method, form the basis of most widely used commercial software programs used in the analysis of building structures. Current codes of practice for building structures mandate the use of methods that consider geometric nonlinearity. For example, the AISC specification requires that the second-order nonlinear effects of $P-\Delta$ and $P-\delta$ be included in the analysis and design of steel structures via the code-specified "Direct Analysis Method". [13] The Eurocode also mandates the inclusion of second-order deformations with similar methodologies in the stability design of frames. [14]

While several factors, such as the slenderness of columns and stiffness of beams, mainly affect the stability of steel frames, the effects of the rigidity of connections between columns and beams on stability are typically overlooked. In practice, when modelling structures, all moment connections are often assumed fully rigid, transferring full moments and rotations of the beam to the column, and all shear connections are assumed purely hinged, isolating beam rotations and moments from the column. However, experiments have consistently shown that connections typically exhibit semi-rigid behaviour lying somewhere between fully rigid and purely hinged. Factors such as bolt size, connecting plate thickness, and framing angles, among several other factors, have been known to critically influence the stiffness of connections. [15-19]

Thus, the ongoing practice of idealizing joints as either pinned or rigid and ignoring their actual stiffness in structural analysis can lead to considerably inaccurate results. Several studies have been conducted to capture connections' behaviour, and various empirical formulas have been proposed to fit their experimental moment-rotation curves. A summary of these formulas and their historical development can be found in [16, 20]. Moreover, attempts have been made to compile all available experimental data of various types of steel connections into database programs. [21] These programs enable the user to extract the moment-rotation characteristics, based on a given connection configuration, which can then be used in modelling joints properly when analysing structures.

On analysis of structures, efforts were made to devise methods that account for the flexibility of connections in the structural model. For example, [22] developed stiffness matrices using an updated Lagrangian formulation for beam-column elements with springs at their ends. Then, by using these formulations, a toggle snap-through structural system with flexible supports was analysed and was found to experience appreciably more deflections than the case with rigid supports. In the same study, a four-storey steel frame structure with semi-rigid steel connections modelled through springs experienced lateral drifts 10.9% greater than its rigidly connected counterpart. The numerical procedures and techniques used in the study were detailed in another paper. [23] Others used iterative numerical approaches to investigate the effect of the fixity of joints on the critical buckling load of braced and unbraced frames and concluded that the buckling capacity of frames could significantly increase for a marginal increase in the degree of fixity of joints. [24] The results were also validated using an experimental apparatus devised in the same research, and it was found that the proposed analytical method overestimated the experimental critical buckling load by 19%. A different numerical treatment for analysing semi-rigid frames, relying on power series expansions of the stiffness equations, was proposed to eliminate numerical difficulty under small axial forces and allow unified treatment for tensile and compressive forces. [25] While all these studies considered stability via geometric nonlinearity [22-24], other studies focused on the first-order behaviour of steel frames with semi-rigid joints. [26-28] In general, there is a consensus among researchers in the field on the necessity of incorporating joints' stiffness in the analysis of structures, particularly when stability is a concern.

Although the methods proposed in the literature are all numerical and account for connections' flexibility, they serve different purposes. Some methods aim to trace the nonlinear load-deformation response [22,23], while others investigated the effect of joint semi-rigidity on straining actions. [25,28] Little research was found on determining the critical buckling load value of semi-rigid frames. [24]

The numerical methods presented so far pose two main problems: (1) they are approximate numerical methods that do not readily reveal the critical buckling load or the parameters controlling stability; and (2) they are computationally intensive due to the incremental and iterative schemes used. The first problem can only be overcome by providing a mathematical treatment that reveals the key parameters

controlling stability and how they are related. To the authors' knowledge, no analytical study was found in the existing body of literature that mathematically investigated the effect of joint flexibility on the critical buckling load. Thus, this paper's first objective is to set a theoretical framework from first principles for calculating the exact critical buckling load with no approximations and for identifying the key parameters governing the stability of frames having semi-rigid joints.

To address the second problem, this paper introduces stableX, a program that was developed to perform efficient numerical analysis of flexibly jointed structures. The program implements a non-iterative one-step eigenvalue analysis technique to calculate the critical buckling load with high accuracy. The proposed numerical method not only confirms theoretical predictions with high precision but can also capture higher modes of buckling effectively, allowing critical loads for both braced and unbraced frames to be computed at the same time without recalculations. The last objective of this paper is to measure the effect of code-classified semi-rigid connections (to the AISC and Eurocode provisions) on the buckling capacity of frames using the methods devised herein. Additionally, to demonstrate the utility of the analytical method, the effect of column base flexibility on the structural stability is briefly explored.

To ensure the applicability and reliability of the proposed methods, the following assumptions are adopted:

- Material elasticity: It is assumed that the materials used in the structures are perfectly elastic.
- Plane buckling restriction: The analysis restricts buckling to within the plane of the frame, thereby excluding out-of-plane buckling phenomena from consideration.
- Small deflection: Deflections are considered small, allowing the use of approximate curvature expressions. $EI\ d^2y/dx^2 = -M$. This assumption is a precursor to the development of all readily available stability functions.

2. Analytical Methodology

In the mathematical treatment, it is hypothesized that there exist non-dimensional key parameters that control the buckling capacity of frames with flexible joints. The terms "flexible" and "semi-rigid" are used interchangeably herein, aligning with the literature, in describing joints that are neither fully rigid (i.e., transmit full rotations and moments) nor fully pinned (i.e., transmit zero moments or rotations) but that possess finite stiffness (i.e., transmit moments and rotations partially). To reveal these parameters, classical stability functions are employed. The methodology is demonstrated through its application to a single-storey rectangular frame, analyzed in two scenarios: sway-permitted and sway-prevented (i.e., braced). By following this method, one arrives at the governing buckling equation that contains the key controlling parameters of the structure's stability. Since stability functions form the foundation of the present work, a brief overview is provided. Stability functions are analogous to the ordinary slope-deflection coefficients. In the ordinary slope-deflection method, a stiffness coefficient represents the force or moment needed to induce unit displacement or rotation at a specific degree of freedom in the element under no axial load while holding the other degrees of freedom fixed. In this case, the resulting equilibrium differential equations are simple, yielding constant stiffness coefficients. In contrast, to derive stability functions, equilibrium equations are formulated on the deformed state of the element under a sustained axial load. This further complicates the differential equation by adding the term $(P \cdot y)$ or similar variants depending on the boundary conditions, where P and y are the axial load and deflection curve, respectively. This results in stiffness coefficients (i.e., stability functions) that are nonlinear in the axial load P and that involve complex trigonometric expressions. In a frame structure consisting of more than one element, equilibrium is enforced discretely at the joints, thereby resulting in a number of equilibrium equations equal to the number of free degrees of freedom in the overall structure. This system of equilibrium equations typically leads to a symmetric matrix. To obtain the critical load, the determinant of this matrix must be set to zero to have non-trivial solutions for displacements at the critical state. Since the terms in the matrix involve stability functions that depend on the axial load in each element of the frame, a first-order analysis is initially required to determine the axial force distribution across all elements. In doing so, it is assumed that the axial force distribution in the frame remains constant until the point of buckling. [29]

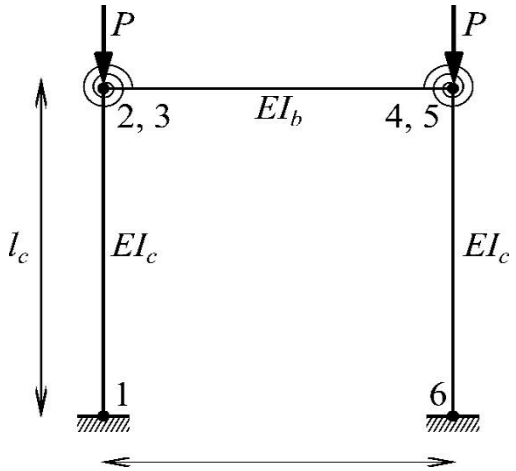

Fig. 1 Frame in the initial undeformed state

To illustrate the method, a single-storey rectangular frame is analyzed. The frame is assumed to be fixed at the base and subjected to concentric point load P on each column, as shown in Figure 1. Joint flexibilities are modelled through rotational springs, each of which has two rotational degrees of freedom, one at each end of a spring. These purely theoretical springs have zero length and extend out of the plane of the frame. They are placed between columns and beams to ensure rotational

incompatibility as dictated by the real connection behavior (see Figures 2 and 3).

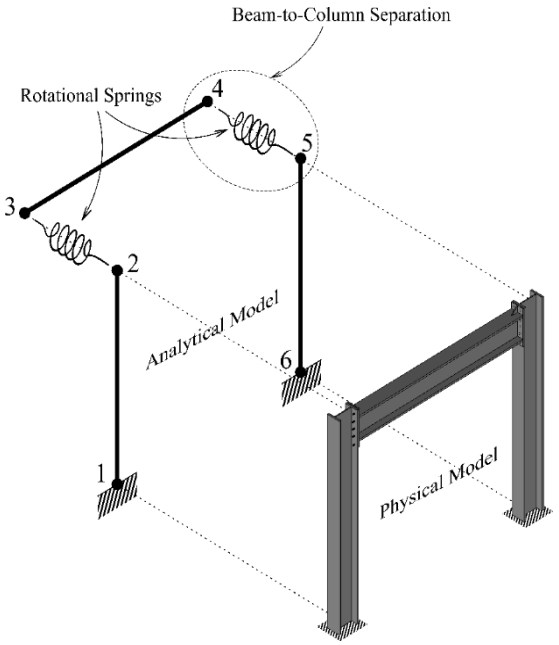

Fig. 2 Analytical representation of a frame having semi-rigid connections

The springs should simulate the rotational stiffness of the actual steel connections. Rotational stiffness is the moment needed to induce unit rotation. A wide survey of literature indicates that the moment-rotation behavior of steel connections is often complex and nonlinear. [15,16,21] Despite this inherent nonlinearity, several design codes classify connections based on either their secant stiffness at a given applied moment [13] or their initial tangent stiffness. [30] Assigning to springs a constant stiffness value (i.e., secant or initial tangent) will prove helpful in the analytical investigation, as this allows the derivation of parameterized equations that offer insight into the stability of semi-rigid frames, as demonstrated next.

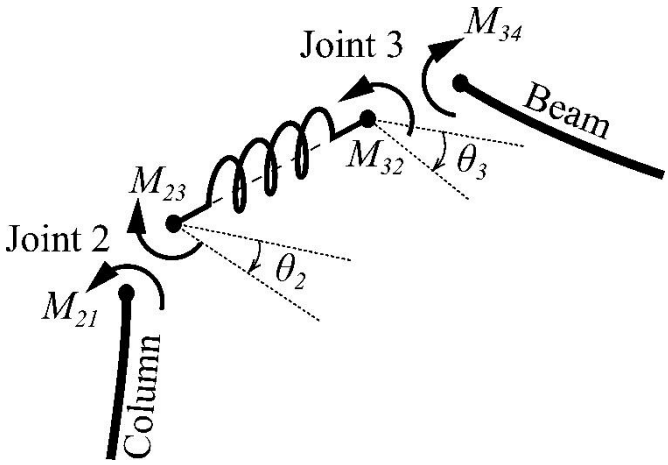

Fig. 3 Rotational spring element separating the column from the beam

Let $K_c = EI_c/l_c$, $K_b = EI_b/l_b$, and K_s be the bending stiffness of columns, the beam, and the spring constant, respectively. Where E is the modulus of elasticity, I_c and I_b are the moments of inertia for columns and beam cross-sections, and l_c and l_b are as shown in Figure 1.

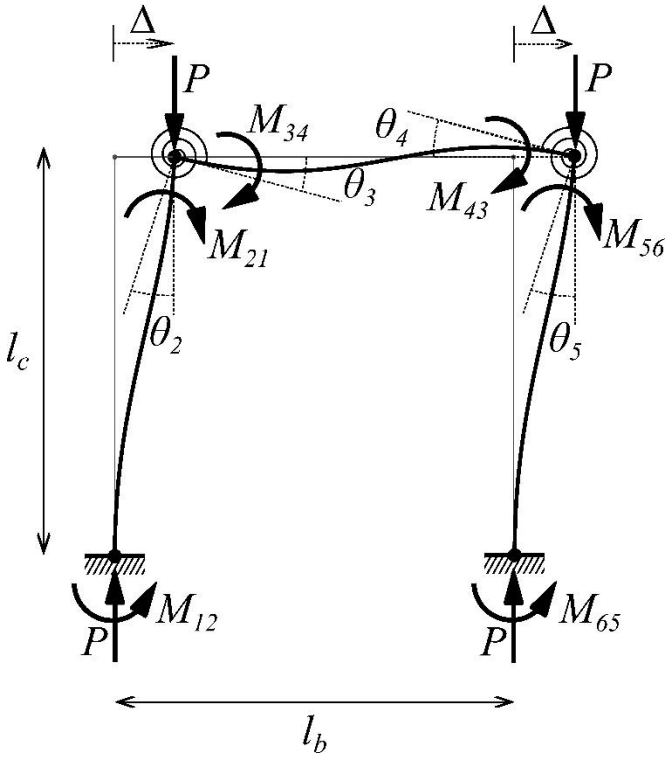

Fig. 4 Frame in the buckled state with end moments indicated

Under the shown loading conditions, each column carries an axial load P. Due to the symmetry of the loading, geometry, and boundary conditions, the frame buckles in anti-symmetrical no-shear sway mode, as depicted in Figure 4. Consequently, the beam is free from axial forces. Therefore, stability functions are solely applicable to the equations at the column ends. In this anti-symmetrical buckling mode, two equilibrium equations need only be formulated, one at each end of the spring: the equilibrium equation of moments at the column-to-spring junction at Joint 2, and the equilibrium equation of moments at the spring-to-beam junction at Joint 3, shown in Figure 3. First, the elements' end moments shall be expressed as follows:

The column end moment at Joint 2 is:

$$M_{21} = nK_c\theta_2 \tag{1}$$

Where n is a stability function derived for the case of no-shear sway buckling of columns and is rewritten here for reference: [6]

$$n = \mu l_c \cot(\mu l_c) \tag{2}$$

$$\mu = \sqrt{\frac{P_{cr}}{EI}} \quad \rightarrow \quad \mu l_c = \pi \sqrt{\frac{P_{cr}}{P_E}} = \pi \sqrt{\rho} \tag{3}$$

Where P_{cr} is the critical buckling load of the frame, and ρ is the critical load ratio defined as $\rho = P_{cr}/P_E$. Euler's critical load, P_E, is expressed as: [3]

$$P_E = \pi^2 \frac{EI_c}{l_c^2} \tag{4}$$

The spring torsional moments are:

$$M_{23} = -M_{32} = K_s\theta_2 - K_s\theta_3 \tag{5}$$

The beam end-moment in the absence of axial forces is also known:

$$M_{34} = 4K_b\theta_3 + 2K_b\theta_4 \tag{6}$$

Due to anti-symmetry, $\theta_3 = \theta_4$. Therefore, Equation (6) may be written as:

$$M_{34} = 6K_b\theta_3 \tag{7}$$

Equilibrium equations of moments can then be written for Joints 2 and 3 as follows:

$$\sum M_2 = 0 \quad \rightarrow \quad M_{21} + M_{23} = 0 \tag{8}$$

$$\sum M_3 = 0 \quad \rightarrow \quad M_{32} + M_{34} = 0 \tag{9}$$

Substituting Equations (1), (5), and (7) in (8) and (9):

$$nK_c\theta_2 + K_s\theta_2 - K_s\theta_3 = 0 \tag{10}$$

$$-K_s\theta_2 + K_s\theta_3 + 6K_b\theta_3 = 0 \tag{11}$$

Equations (10) and (11) are then cast in matrix form:

$$\begin{bmatrix} nK_c + K_s & -K_s \\ -K_s & K_s + 6K_b \end{bmatrix} \begin{Bmatrix} \theta_2 \\ \theta_3 \end{Bmatrix} = 0 \tag{12}$$

Non-trivial solutions for the displacement vector in Equation (12) exist if, and only if, the determinant vanishes, that is:

$$(nK_c + K_s)(K_s + 6K_b) - K_s^2 = 0 \tag{13}$$

By expanding Equation (13) and dividing by K_cK_s:

$$6\frac{K_b}{K_c} + 6n\frac{K_b}{K_s} + n = 0 \tag{14}$$

Equation (14) can be solved numerically for the critical buckling load of sway-permitted frames for any beam-to-column K_b/K_c and beam-to-spring K_b/K_s relative bending stiffness ratios. For the case of braced (sway-prevented) frames, Figure 5 shows a schematic of their typical buckling mode. In this case, the stability function s shall be used instead of n: [6]

$$s = \mu l_c \frac{\sin(\mu l_c) - \mu l_c \cos(\mu l_c)}{2 - 2\cos(\mu l_c) - \mu l_c \sin(\mu l_c)} \tag{15}$$

Frames prevented from swaying (i.e., braced) buckle in a symmetrical mode shape such that the beam end rotations are equal in magnitude but opposite in direction, i.e., $\theta_3 = -\theta_4$. This slightly modifies the previous formulation, resulting in factor 2 replacing 6 in Equation (14). Therefore, the critical buckling load equation for braced frames becomes:

$$2\frac{K_b}{K_c} + 2s\frac{K_b}{K_s} + s = 0 \tag{16}$$

A detailed discussion of the significance and implications of Equations (14) and (16) is provided in Section 4 of this paper. Additionally, formulations for the case of semi-rigid and hinged bases are presented in the same section.

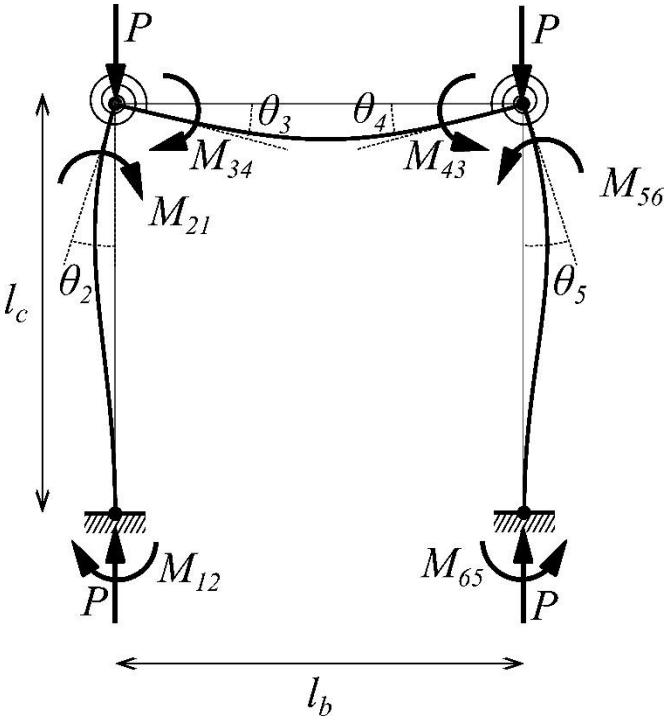

Fig. 5 Frame in the buckled state with end moments indicated

3. Numerical Analysis through the Custom Software stableX

A Python program, "stableX", was developed for the purpose of this research to achieve two main objectives: to verify the mathematical treatment proposed in this paper and to establish a generalized framework that enables fast and efficient stability analysis of flexibly jointed structures with more complex geometry, loading, and boundary conditions.

stableX is designed on Object-Oriented Programming (OOP) principles to enhance usability for the end user, meaning that entities such as degrees of freedom, nodes, elements, and loads are treated as objects in the programming paradigm. This design not only allows the addition of different types of elements, such as rotational or linear springs and bar elements, to its library, but also allows incorporating different types of analysis, such as first-order elastic analysis and eigenvalue buckling analysis, all of which are central in analyzing structures having semi-rigid joints. stableX also provides visualization through the library "Matplotlib". (For reproducibility of the results presented in this paper, the developed program, stableX, was made open-source and is licensed under the MIT License. The source code is available at https://github.com/Hazem-Kassab/stableX, and the package can be installed directly via the Python Package Index at https://pypi.org/project/stableX/.

3.1. Elements' Stiffness Matrices

Two types of elements are used in this study: the frame element, which has six degrees of freedom, and the spring element, which has two rotational degrees of freedom. For the frame element, the program employs the ordinary elastic stiffness matrix $[k_e]$ and the typical geometric stiffness matrix $[k_g]$ which accounts for geometric nonlinearities and second-order effects, as represented by Equations (17) and (18), respectively: [7, 12, 29]

$$[k_e] = \begin{bmatrix} \frac{EA}{L} & 0 & 0 & -\frac{EA}{L} & 0 & 0 \\ 0 & \frac{12EI}{L^3} & \frac{6EI}{L^2} & 0 & -\frac{12EI}{L^3} & \frac{6EI}{L^2} \\ 0 & \frac{6EI}{L^2} & \frac{4EI}{L} & 0 & -\frac{6EI}{L^2} & \frac{2EI}{L} \\ -\frac{EA}{L} & 0 & 0 & \frac{EA}{L} & 0 & 0 \\ 0 & -\frac{12EI}{L^3} & -\frac{6EI}{L^2} & 0 & \frac{12EI}{L^3} & -\frac{6EI}{L^2} \\ 0 & \frac{6EI}{L^2} & \frac{2EI}{L} & 0 & -\frac{6EI}{L^2} & \frac{4EI}{L} \end{bmatrix} \quad (17)$$

Where E, I, and A are the modulus of elasticity, moment of inertia, and area of the element cross-section, respectively, while L is the length of the element.

$$[k_g] = \frac{N}{L}\begin{bmatrix} 1 & 0 & 0 & -1 & 0 & 0 \\ 0 & \frac{6}{5} & \frac{L}{10} & 0 & -\frac{6}{5} & \frac{L}{10} \\ 0 & \frac{L}{10} & 2\frac{L^2}{15} & 0 & -\frac{L}{10} & -\frac{L^2}{30} \\ -1 & 0 & 0 & 1 & 0 & 0 \\ 0 & -\frac{6}{5} & -\frac{L}{10} & 0 & \frac{6}{5} & -\frac{L}{10} \\ 0 & \frac{L}{10} & -\frac{L^2}{30} & 0 & -\frac{L}{10} & 2\frac{L^2}{15} \end{bmatrix} \quad (18)$$

The geometric stiffness matrix $[k_g]$ is linear in N (the internal axial force), this linearization is a result of the Taylor series expansion of stability functions truncated after the first two terms. This approximation provides accurate results if members are divided into sufficiently small elements to ensure that the ratio P/P_{cr} does not exceed 0.1 for each element. This ratio corresponds to the range (0 to 0.1) where stability functions can be approximated as linear with insignificant error. [29] Unlike stability functions, which need to be reformulated as hyperbolic functions when the element is under tension [29], the geometric stiffness matrix (Equation (18)) remains valid in tension. [7] This is because Taylor's expansion of the hyperbolic counterparts is the same as those derived for compression, with the key difference being an alternating sign applied from the second term onward. When N is negative, it signifies compression, resulting in a decrease in total stiffness and indicating potential instability. Conversely, a positive N signifies tension, which increases the total stiffness and contributes to stabilizing the element.

The rotational spring element used in the program possesses the following stiffness matrix:

$$[k_s] = K_s \begin{bmatrix} 1 & -1 \\ -1 & 1 \end{bmatrix} \quad (19)$$

While the stiffness of springs could be incorporated directly into the stiffness matrix of the frame element by static condensation, a method adopted by several studies [22-26], stableX models springs as distinct elements in the structure, as illustrated in Figure 2. This facilitates the placement of spring elements at any specific location in the structure, or their complete removal when full fixity is required. Embedding springs in frame elements would necessitate assigning excessively large stiffness values to approximate full fixity, which is less straightforward and less accurate. Additionally, separate stiffness matrices must be formulated for the cases of frame elements with a spring at one end, both ends, or neither end; these then would have to be added to the elements' library inside the program.

The approach taken in stableX in modelling springs as separate elements offers several advantages: it allows the direct use of the standard textbook formulations of the elastic and geometric stiffness matrices (Equations (17) and (18)) without the need for rederiving modified stiffness matrices for frame elements incorporating springs at their ends. This can potentially be useful for existing finite-element packages since only the separate spring stiffness matrix needs to be programmed into the software library. Additionally, the spring element implementation in the software is such that rotational Degrees Of Freedom (DOFs) at the spring ends are decoupled while translational DOFs at both ends point to the same object in memory (i.e., coupled), simulating the effect of joint rotational flexibility effectively. The object-oriented nature of stableX also facilitates the development of different implementations of the spring element, enabling the incorporation of other axial and lateral DOFs in addition to the rotational DOFs in springs. Such spring elements can then be seamlessly integrated into the software library to better

capture other dimensions of deformability in the connection. Furthermore, the coupling techniques available through the program's design make use of memory efficiently and eliminate unnecessary increases in degrees of freedom, which enhances the program's capability to analyze structures with semi-rigid joints effectively.

3.2. Eigenvalue Analysis for Critical Buckling Load Determination

Several methods exist for buckling analysis. On the one hand, there are incremental methods that consider geometric nonlinearity and, in some cases, material nonlinearity. These techniques include multi-step iterative processes in which the load is incremented gradually until excessive deformations occur or the stiffness matrix determinant approaches zero, indicating instability. On the other hand, eigenvalue buckling analysis, adopted in this paper, is a non-iterative single-step procedure for calculating buckling loads. This method of analysis not only offers a fast and efficient means of calculating the critical loads but also captures higher modes of buckling effectively. Unlike incremental methods, which require imposing specific boundary conditions or otherwise tweaking imperfections in such a way as to induce a specific buckling mode shape, eigenvalue analysis allows for both braced and unbraced frames to be analysed using the same model and matrix formulation by simply extracting the first and second computed eigenpairs, respectively, in a single step without recalculations. The developed package, stableX, performs eigenvalue buckling analysis through a sequence of procedures. It begins by performing a first-order analysis to determine the axial force distribution in the structure's elements. This process starts with the formulation of the elastic stiffness matrix $[k_e]$ for each element in the structure. The elements' stiffness matrices are then transformed from local to global coordinate systems through coordinate transformations $[T]$. Next, the global elastic stiffness matrix, $[K_E]$. The structure is assembled by combining the elements' transformed matrices. Once assembled, the global stiffness matrix is partitioned to solve for the unknown displacements. Nodal forces $\{f\}$ within all elements are then computed using the obtained end displacements of each member. Once the axial forces N in the elements are known, the global geometric stiffness matrix, $[K_G]$, of the structure is then assembled and partitioned in a similar manner. Finally, an eigenvalue problem is formulated and solved to determine the critical loads and their associated mode shapes. The overall analysis procedure is illustrated in the flowchart shown in Figure 6, and its implementation is provided in the source code. To formulate the eigenvalue problem, the equations of equilibrium at the free degrees of freedom must first be expressed in incremental form, which is written in matrix notation as:

$$\left([K_E]_{ff} + [K_G]_{ff}\right)\{d\Delta\} = \{dF\} \tag{20}$$

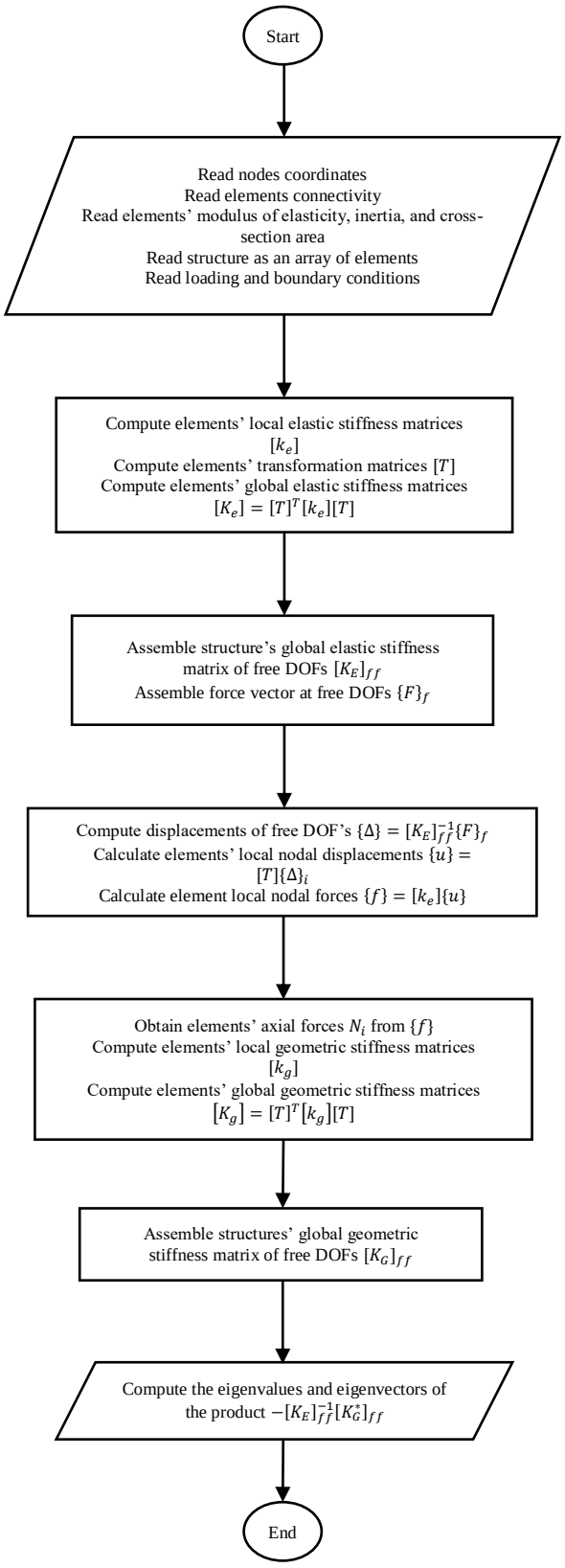

Fig. 6 Flowchart of the buckling analysis procedure in stableX

Where:

- $[K_E]_{ff}$ and $[K_G]_{ff}$ are partitions of the assembled global elastic and global geometric stiffness matrices corresponding to the free degrees of freedom, respectively. The sum $[K_E]_{ff} + [K_G]_{ff}$ represents the tangent stiffness matrix.
- $\{d\Delta\}$ is the displacement increment, and $\{dF\}$ is the load increment at the free degrees of freedom.

The axial force N_i for any element i in the framework, obtained from first-order analysis, can always be expressed as some multiple α_i of the applied load P (i.e. $N_i = \alpha_i P$). Consequently, the local geometric stiffness matrices (Equation (18)) of all elements can be expressed in terms of P. It follows that the multiplier P can be factored out in the global geometric stiffness matrix, i.e., $P[K_G^*]_{ff}$.

Thus, Equation (20) can be rewritten as:

$$\left([K_E]_{ff} + P[K_G^*]_{ff}\right)\{d\Delta\} = dF \tag{21}$$

The critical state can then be sought for non-trivial displacements under vanishing load increment: [20]

$$\left([K_E]_{ff} + P[K_G^*]_{ff}\right)\{d\Delta\} = 0 \tag{22}$$

Expanding and rearranging Equation (22) yields:

$$-[K_E]_{ff}^{-1}[K_G^*]_{ff}\{d\Delta\} = \frac{1}{P}d\Delta \tag{23}$$

Equation (23) is a standard eigenvalue problem that can be expressed as:

$$\left(-[K_E]_{ff}^{-1}[K_G^*]_{ff} - \lambda[I]\right)\{d\Delta\} = 0 \tag{24}$$

In Equation (24), $\lambda = 1/P$, and $[I]$ is the identity matrix of size equal to the number of free degrees of freedom. The inverses of the eigenvalues are the critical buckling load multipliers, while the eigenvectors represent the buckling mode shapes associated with the eigenvalues. The Python package "NumPy" is employed in the program to compute the eigenpairs of the product $-[K_E]_{ff}^{-1}[K_G^*]_{ff}$. The number of buckling mode shapes and their associated critical loads is equal to the number of free degrees of freedom in the system. Unlike the iterative nature of the numerical techniques used in the literature, "Numpy" utilizes non-iterative QR factorization schemes to deterministically find all the eigenvalues and eigenvectors in a finite number of steps, yielding accurate results with high computational efficiency. [31]

3.3. Verification of stableX

In this section, stableX is verified against benchmark problems in stability. Two problems are investigated: (1) the classical Euler's pinned column, shown in Figure 7(a), and (2) the rigid bar and spring assembly, shown in Figure 7(b); both of which have well-known solutions. These classical problems were specifically selected to adequately verify the capabilities of stableX in analyzing flexural buckling and accounting for joint flexibility. The theoretical solution to the pinned column problem is well-documented in the literature: [1-4,29,32]

$$P_{cr} = n^2\pi^2\frac{EI}{l^2} \tag{25}$$

Where n is a positive integer reflecting the buckling mode shape, E and I are the column's elasticity modulus and cross-sectional inertia, respectively, and l is the column's length. Substituting $n = 1$ in Equation (25) yields Equation (4), which corresponds to the lowest buckling mode of a half-sine wave. The theoretical solution to the second problem of the rigid bar and spring system is as follows: [2, 33]

$$P_{cr} = \frac{k}{l} \tag{26}$$

Where k is the spring constant and l is the bar length.

Equations (25) and (26) will provide benchmarks for comparison against results from stableX. The following presents examples of the two problems: (The Python scripts used to model these problems in stableX are available at https://github.com/Hazem-Kassab/stableX/tree/master/verification_problems)

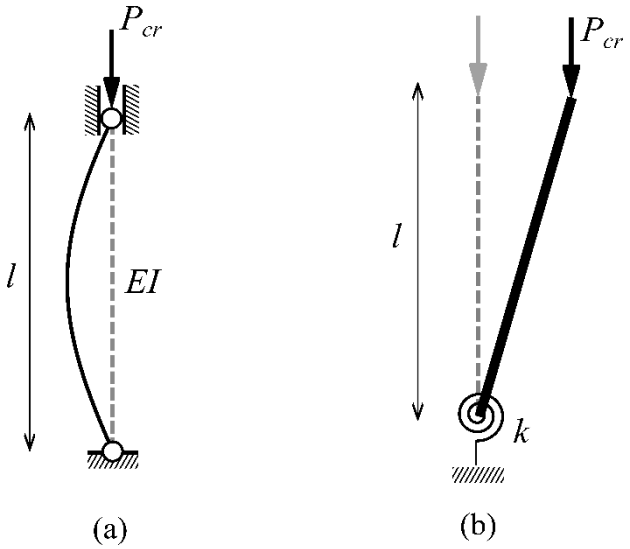

Fig. 7 Classical benchmark buckling problems of (a) Pinned column, and (b) Rigid bar and spring assembly.

Problem 1: Consider a 6-m-long pinned column subjected to axial compression. The column has profile IPE200 with properties: $A = 53.8\ \text{cm}^2$, $E = 200 \times 10^3$ MPa and $I = 1340\ \text{cm}^4$ (weaker axis). The critical loads calculated through Equation (25) are 77.86 kN for the first mode ($n = 1$) and 311.44 kN for the second mode ($n = 2$). In $stableX$, the column was modelled with a mesh of four frame elements

having the same profile and material properties mentioned previously. Analysis was then performed, and the first two eigenpairs were extracted. Figure 8 shows the resulting mode shapes and the corresponding buckling loads computed by stableX: 77.9 kN and 313.78 kN for the first and second modes, respectively. It is evident that the results from stableX are in strong agreement with the results obtained theoretically from Equation (25), with very small discrepancy; error less than 0.05% for the first mode and less than 0.75% for the second mode. In general, error increases with higher modes of buckling due to the increase in the ratio P_{cr}/P_E for elements at higher buckling loads. To circumvent this, a more refined mesh might be necessary at higher buckling modes.To ensure adequate verification of stableX, the length of the column was varied in half-meter increments in the program, and the corresponding critical loads for first and second modes were computed at each increment. Figure 9 presents a chart comparing the results with Equation (25). The chart indicates that stableX predicts the flexural buckling loads with high precision.

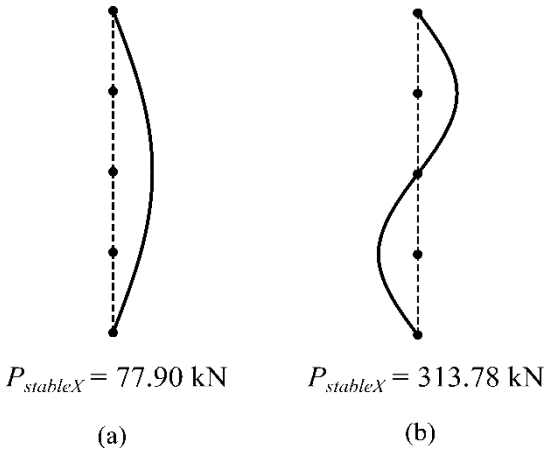

Fig. 8 stableX output for the buckling mode shapes and their corresponding critical loads, (a) First mode, and (b) Second mode.

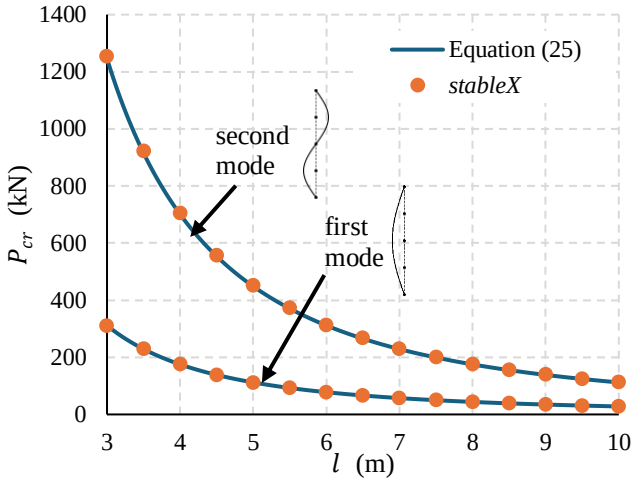

Fig. 9 Comparison between stableX and the theoretical solution for the buckling of the pinned column

Problem 2: Consider a 2-m rigid bar free at the top and connected to a fixed base via a rotational spring having constant $k = 20$ kN.m/rad. Substituting these inputs in Equation (26) yields the exact critical load value of 10 kN. To model the system in stableX, a single frame element with a very large cross-sectional area was used to simulate the rigid bar, and a linear rotational spring element was used to connect the bottom node of the bar to the fixed base node. The analysis in stableX yielded the mode shape depicted in Figure 10 and a critical buckling load of 10 kN, matching the theoretically predicted value exactly to two decimal places. Figure 11 is a chart showing the strong agreement between stableX and Equation (26) in solving problem 2 for different bar lengths. The plot verifies the program's ability to analyse semi-rigid joints efficiently and accurately. Having verified stableX, the next section investigates a single-storey steel frame with semi-rigid joints.

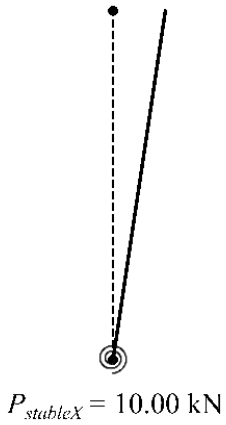

Fig. 10 stableX output for the buckling mode of the rigid bar and the corresponding critical load

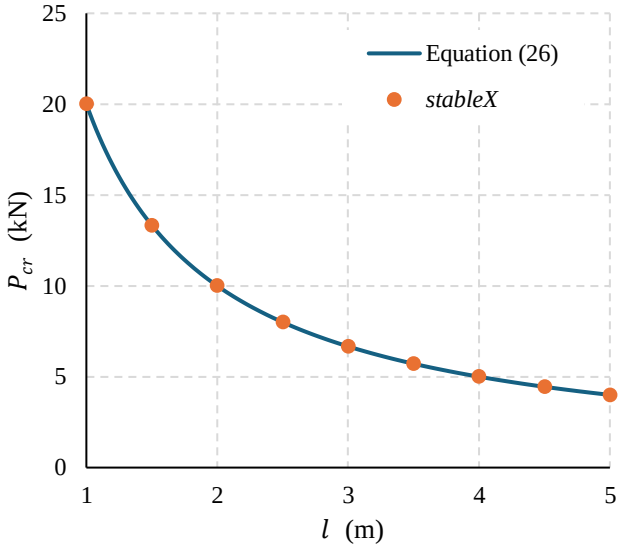

Fig. 11 Comparison between stableX and the theoretical solution for the buckling of the rigid-bar and spring assembly

3.4. Numerical Modelling of a Single-Storey Rectangular Frame in stableX

To verify Equation (14), a single-storey 11 m × 11 m steel frame is modelled. Figure 12 illustrates the model in its initial undeformed configuration, the end boundary conditions, the loading pattern, and element meshing of the frame. Unit loads are applied to the frame so that by inverting the resulting eigenvalues, the critical buckling loads are directly obtained.

The columns are discretized into six elements to ensure that the critical load ratio P_{cr}/P_E for each element, the value remains less than 1/36 in the case of sway buckling and less than 1/9 if braced. This guarantees that the ratio P_{cr}/P_E is sufficiently small, lying in the range where stability functions can be approximated as linear and ensuring accurate results. [29] While such fine discretization significantly increases the degrees of freedom and is unnecessary for most practical scenarios, this refined mesh is justified in this paper for precise verification of the analytical results. In fact, modelling each column as a single unmeshed element results in a maximum error of only 1.05% in this example.

Table 1. Properties of the profiles used in the numerical and analytical analysis

Profile	A (cm^2)	I (cm^4)
IPE160	20.09	869.3
IPE200	28.48	1943
IPE240	39.12	3892

The analysis was conducted on the frame with different combinations of profiles for the beam and columns, selected from the European profiles IPE160, IPE200, and IPE240. S355 steel grade was assigned to all members, with a yield strength of 355 MPa and an elasticity modulus of 210 GPa. These selected profiles ensure elastic buckling failure by maintaining a critical stress below 44% of the yield strength, in accordance with the AISC provisions [13], which aligns with the assumptions of this research. Table 1 presents the profile properties used in the numerical and analytical analyses.

In the analysis, for each set of beam and column profiles, the spring stiffness was varied using multiples of 0, 2, 5, 20, and ∞ relative to the beam's bending stiffness K_b. The selected ratios K_b/K_s ranging from 1/20 to 1/2 fall within the range where connections are classified as semi-rigid under service loads, with K_s representing the secant stiffness of the connection's $M-\theta$ curve, as per the AISC specification. [13]

3.5. Comparison with the Exact Solution

Table 2 presents the critical loads obtained from the stiffness method in stableX for the frame with various beam and column profile combinations. It is evident that as the spring stiffness decreases from the top to the bottom of the table, the frame's critical load decreases substantially. The strong agreement between the analytical predictions and the stiffness method verifies the analytical approach and all its underlying assumptions. In all cases, the lowest buckling load of the frame corresponds to a typical sway-buckling mode, illustrated by the stableX output in Figure 13, as predicted theoretically. Similarly, the second buckling mode, associated with the braced scenario, is depicted in Figure 14.

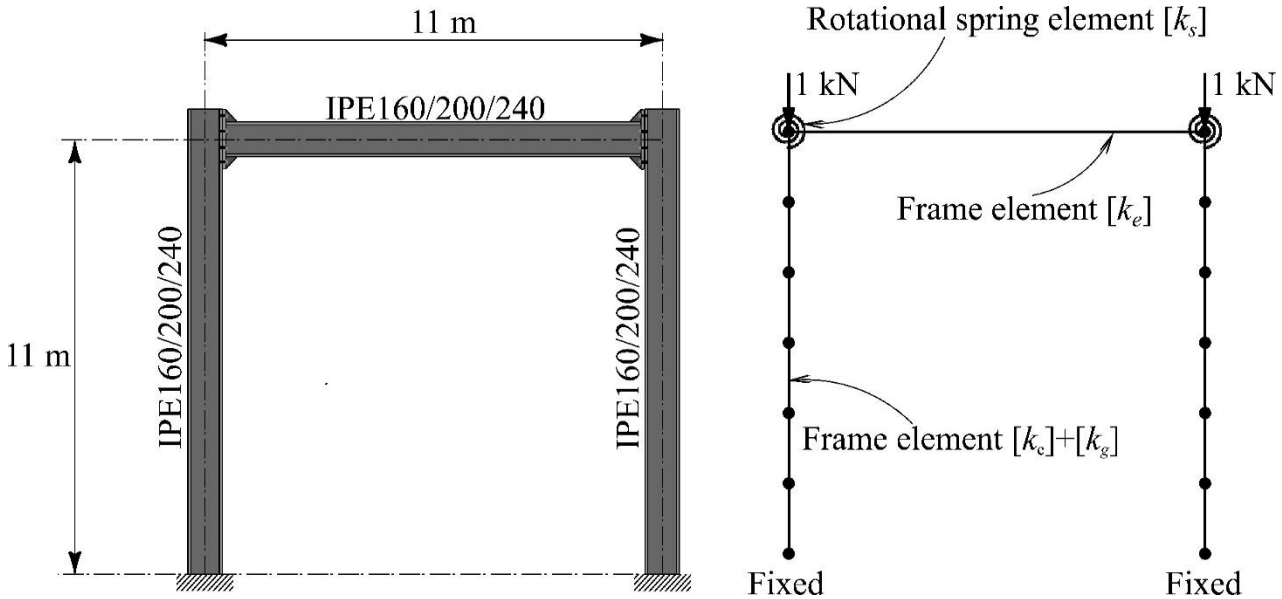

Fig. 12 Elements used in the verification frame model and their associated stiffness matrices in stableX

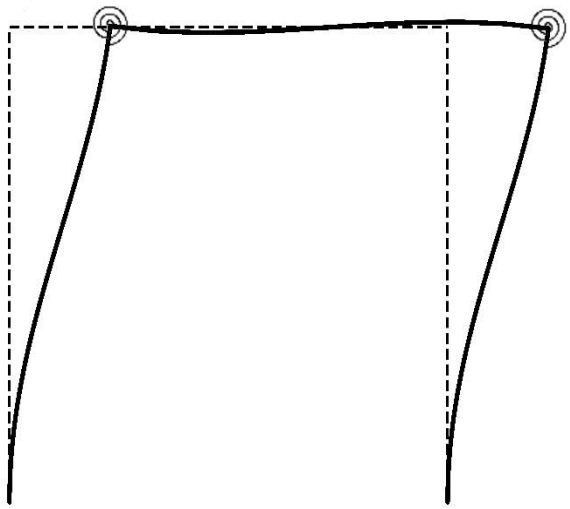

Fig. 13 Typical first buckling mode in stableX

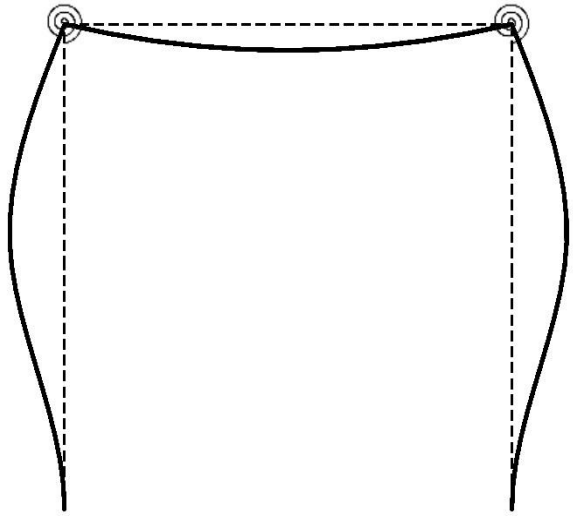

Fig. 14 Typical second buckling mode in stableX

Table 2. Comparison between the results of the stiffness method and the exact solution (loads are in kN)

Column	IPE160			IPE200			IPE240		
Beam	stableX	Eq. 14	Error	stableX	Eq. 14	Error	stableX	Eq. 14	Error
	$K_s = \infty$ (i.e. rigid)								
IPE160	111.31	111.33	-0.02%	195.82	195.86	-0.02%	306.98	307.02	-0.01%
IPE200	129.21	129.23	-0.02%	248.77	248.84	-0.03%	406.99	407.11	-0.03%
IPE240	138.42	138.45	-0.02%	284.38	284.47	-0.03%	498.22	498.44	-0.04%
	$K_b/K_s = 1/20$								
IPE160	103.91	103.92	-0.01%	178.67	178.69	-0.01%	280.78	280.80	-0.01%
IPE200	124.27	124.29	-0.02%	232.22	232.28	-0.03%	371.98	372.07	-0.02%
IPE240	135.53	135.56	-0.02%	272.52	272.60	-0.03%	465.10	465.28	-0.04%
	$K_b/K_s = 1/5$								
IPE160	88.09	88.10	-0.01%	148.37	148.38	-0.01%	239.64	239.65	0.00%
IPE200	111.74	111.76	-0.02%	196.88	196.92	-0.02%	308.68	308.73	-0.02%
IPE240	127.54	127.57	-0.02%	243.00	243.07	-0.03%	394.34	394.45	-0.03%
	$K_b/K_s = 1/2$								
IPE160	71.34	71.35	-0.01%	122.87	122.87	0.00%	209.00	209.00	0.00%
IPE200	94.34	94.35	-0.01%	159.45	159.47	-0.01%	254.02	254.04	-0.01%
IPE240	114.29	114.31	-0.02%	203.41	203.45	-0.02%	319.38	319.43	-0.02%
	$K_s = 0$ (i.e., hinge)								
IPE160	37.23	37.23	0.00%	83.20	83.20	0.00%	166.67	166.67	0.00%
IPE200									
IPE240									

The minor discrepancies between stableX and Equation (14) can be attributed to two reasons: first, the approximation inherent in the formulation of the geometric stiffness matrix of Equation (18) gives rise to some error, since the terms in the matrix are linearizations of the exact stability functions. The second reason is that, unlike stability functions, the stiffness method considers axial deformations in the members. It is essential, however, to recognize that the stiffness method is an approximate extension of the slope-deflection method. While the latter relies on the relative displacement of member end nodes, the former treats each end node displacement separately.

3.6. Analytical Insights and the Effect of Base Flexibility

While the stiffness method proved its versatility, the accuracy and efficiency of the analytical method cannot be overlooked. Studying merely two degrees of freedom has proven not only sufficient but precise, circumventing the need for the lengthier calculations associated with the stiffness method. More importantly, the analytical approach adopted herein abstracts the problem effectively and clearly delineates the critical parameters that govern the bifurcation load, thereby offering a deeper understanding of the structural stability behaviour of structures. Equations (14) and (16) demonstrate that the critical load ratio ρ is not concerned with

the stiffness of columns, beams, or springs; rather, it depends on their relative stiffness ratios. The parameters K_b/K_c and K_b/K_s substantially affect the critical buckling load ratio as illustrated through plots of Equations (14) and (16) in Figures 15 and 16, respectively. The critical buckling load in single-storey sway frames lies within the range $0.25P_E \leq P_{cr} \leq P_E$, where P_E is the Euler buckling load of the columns as defined in Equation (4). This means that the strength of columns in sway frames with rigid beams can, at best, match their strength as pinned columns if the connection is fully rigid. These bounds increase in magnitude and expand in range such that $2.045P_E \leq P_{cr} \leq 4P_E$ for braced frames. The maximum load of $4P_E$ also corresponds to the case where these columns are fixed at both ends, rather than pinned.

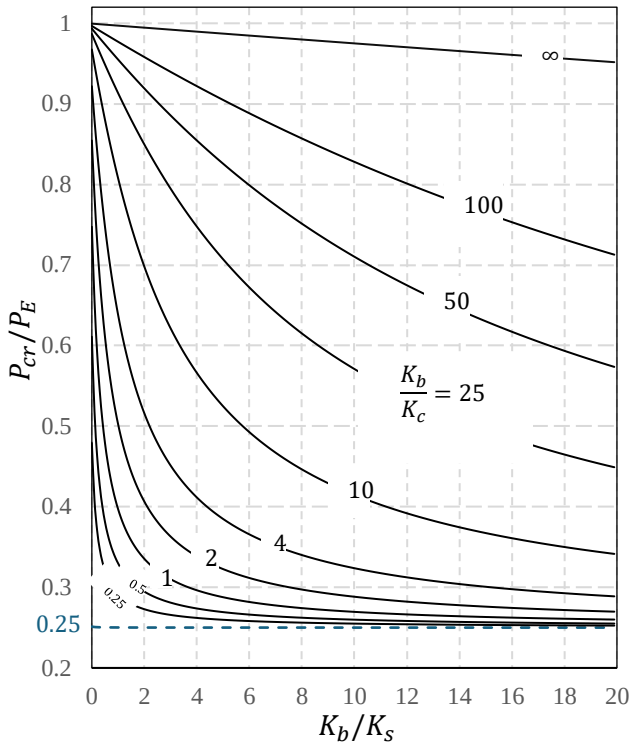

Fig. 15 Effect of beam-to-spring stiffness ratio on the critical load of fixed-base sway frames

Alternatively, the effective length factor, given by $k = 1/\sqrt{\rho}$, offers a more visual perspective of the slenderness of columns in the frame. The effective length factor in unbraced frames varies between $2 \geq k \geq 1$, while for braced frames the range is within $0.7 \geq k \geq 0.5$. These upper bounds, achievable only when connections are fully rigid, are generally lower for practical K_b/K_c ratios. In general, Equations (14) and (16) can be used to determine the maximum critical load or the effective length factor to be used in design for a frame with a specific beam-to-column stiffness ratio.

The plots also reveal significant implications for buckling capacities if moment connections are assumed fully rigid. The steeply declining curves in the lower ranges of K_b/K_s ratios indicate sharp drops in buckling capacity for a small decrease in connection stiffness. For example, steel unbraced frames that have the same profiles for beams and columns, and with K_b/K_s ratio in the range 0 to 1, a common case in practice, experience reductions in capacity of 47% ($\rho = 0.748 \rightarrow 0.397$) when reducing the connection stiffness from ∞ (i.e., fully rigid assumption) to a stiffness equal to that of the beam ($K_b/K_s = 1$).

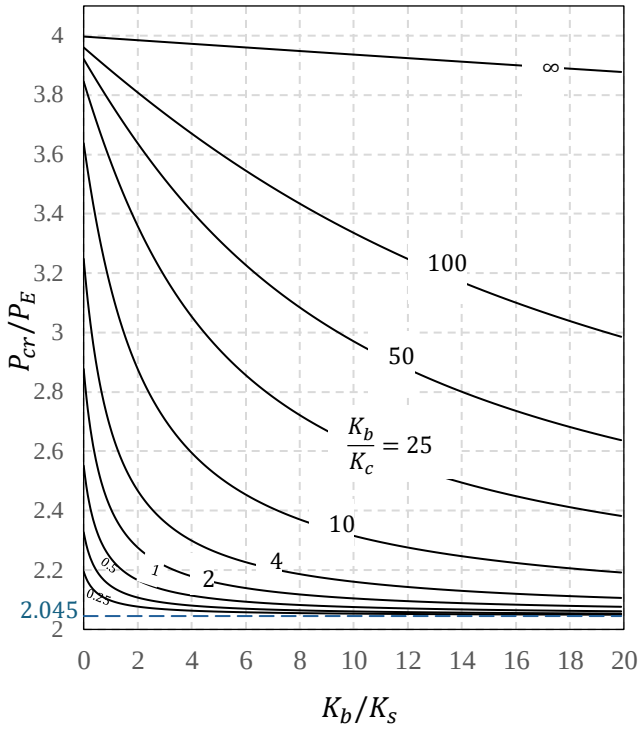

Fig. 16 Effect of beam-to-spring stiffness ratio on the critical load of fixed-base sway-prevented frames

However, the aforementioned bounds for braced and unbraced frames assume idealized base boundary conditions, which are rarely realized. Due to the deformability of the base plates, concrete, and soil, base plates typically exhibit semi-rigid behaviour that lies somewhere between fully fixed and perfectly pinned conditions. [15] This further degrades the stability of steel structures. To account for this, spring elements can be inserted at the column bases too. This generalization, while making the analytical approach more mathematically involved, effectively demonstrates the versatility and applicability to different settings. Equations (14) and (16) then emerge as a special case of a more comprehensive model. The four-spring frame model, schematically illustrated in Figure 17, incorporates semi-rigid connections and bases. The critical buckling load for this generalized model is governed by Equation (27) for sway-permitted frames. If the frame is braced or sway-prevented,

the buckling load is instead governed by Equation (28), which has a similar form to Equation (27). In general, to get the equation for the braced condition, factor 2 replaces 6, s replaces n, and cs replaces o in the unbraced buckling equation. Detailed derivation is provided in Appendix 1.

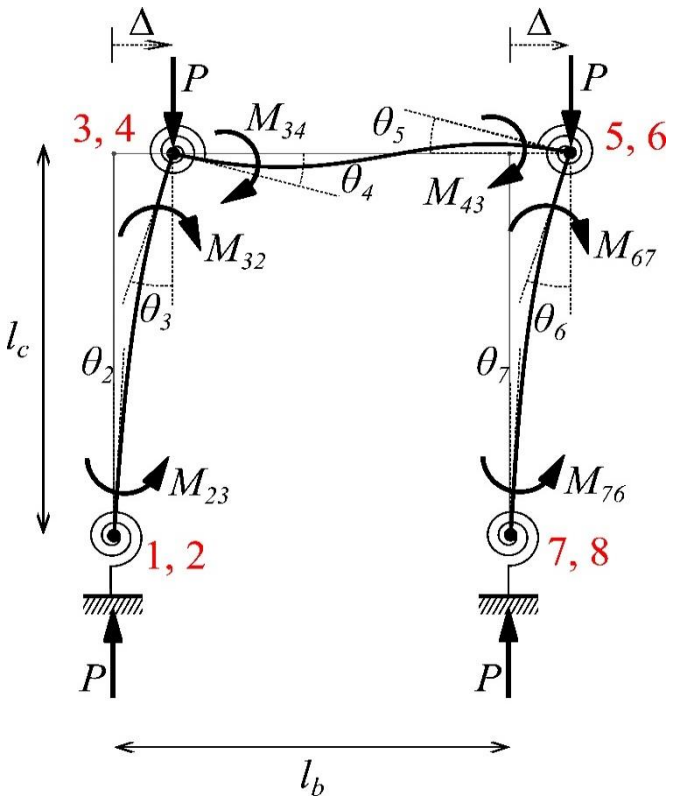

Fig. 17 Four-spring frame model to account for bases and connections' flexibility. Joint labels are highlighted in red.

Unbraced

$$6\beta + n(1 + 6\beta\alpha_1 + 6\alpha_2) + \alpha_1(n^2 - o^2)(1 + 6\alpha_2) = 0 \quad (27)$$

Braced

$$2\beta + s(1 + 2\beta\alpha_1 + 2\alpha_2) + \alpha_1 s^2(1 - c^2)(1 + 2\alpha_2) = 0 \quad (28)$$

Where:

- $\alpha_1 = K_c/K_{s1}$: column-to-base spring stiffness ratio.
- $\alpha_2 = K_b/K_{s2}$: beam-to-connection spring stiffness ratio.
- $\beta = K_b/K_c$: beam-to-column stiffness ratio.
- $o = \mu l_c/\sin(\mu l_c)$: stability function for members with double curvature and subject to sway. [6]
- $c = (\mu l_c - \sin(\mu l_c))/(\sin(\mu l_c) - \mu l_c \cos(\mu l_c))$: stability function representing a carry-over factor. [6]

These generalizations underscore the analytical framework's utility in identifying and isolating the key parameters controlling buckling. This is advantageous when more complex scenarios are encountered and when the factors governing the critical load are obscure, giving more insight into the underlying mechanics of structural stability.

By setting α_1 to zero, the bases become fixed, and Equations (27) and (28) reduce to Equations (14) and (16), respectively. Hinged bases can be modelled by setting $K_{s1} = 0$ in Equations (27) and (28), which, after some algebraic manipulations, lead to the following equations for critical buckling loads of hinged-base frames with semi-rigid connections:

Unbraced

$$6n\beta + (n^2 - o^2)(1 + 6\alpha_2) = 0 \quad (29)$$

Braced

$$2s\beta + s^2(1 - c^2)(1 + 2\alpha_2) = 0 \quad (30)$$

Equations (29) and (30) indicate that the critical load for all single-storey frames with fully rigid connections and hinged bases has an upper limit of $0.25P_E$ when unbraced and $2.045P_E$ when braced. Or an effective length factor of 2 for unbraced frames and 0.7 for braced frames. However, connection springs cannot have zero stiffness when the bases are hinged, as this would result in a statically unstable configuration.

4. Practical Design Considerations

Current codes of practice propose different treatments for the subject of connection flexibility. For example, the AISC specification classifies connections according to their secant stiffness at service loads into three categories: Fully Restrained (FR), Partially Restrained (PR), and simple connections. A PR connection follows the same definition of a semi-rigid connection in this paper. For a connection to be classified as PR to AISC, the secant stiffness K_s must lie within the range $2K_b$ to $20K_b$. AISC requires that PR connections' stiffness, as well as strength and ductility, be included in the analysis. [13] A closer examination of the previous example in Section 3.4 indicates the following: for frames where columns and beams have the same bending stiffness, PR connections result in a reduction of at most 31% in buckling capacity when the connection stiffness is decreased from $20K_b$ to $2K_b$, the range specified in the AISC specification for PR connections. In theory, the percentage change in ρ corresponds directly to the percentage change in P_{cr} This implies that the 31% reduction is universally applicable to all such frames, regardless of the columns' absolute stiffness. For hinged-base frames, Equation (29) yields a greater reduction of 42%. However, only minor reductions in capacity were observed if the frame was braced; 7% reduction for fixed-base braced frames and 9% for hinged-base braced frames. While the AISC specification does not

distinguish between unbraced and braced frames in its criteria for classifying connections, the Eurocode adopts a different approach. The Eurocode provisions specify different limits in braced and unbraced frames for a connection to be classified as semi-rigid. Additionally, the Eurocode bases its criteria on the initial stiffness rather than the secant stiffness of the connection. The Eurocode also requires the behaviour of semi-rigid connections to be accounted for in the analysis. [30]

According to the Eurocode, in unbraced frames, the connection's initial stiffness K_s must fall within the range $0.5K_b < K_s < 25K_b$ to consider the connection as semi-rigid. When K_s decreases from $25K_b$ to $0.5K_b$, Equations (14) and (29) indicate reductions of 53% and 77% in buckling capacity for fixed-base and hinged-base frames, respectively. If K_s exceeds $25K_b$, Eurocode still considers the connection semi-rigid, provided that $K_b/K_c < 0.1$. For braced frames, the range is narrower, specified as $0.5K_b < K_s < 8K_b$, leading to a smaller variation of 12% for fixed-base frames and 17% for hinged-base frames. Table 3 provides a summary of the preceding discussion, where percentage reductions in critical load values correspond to the decrease in connection stiffness from the upper to the lower limit within the specified code range.

Table 3. Buckling capacity variation for frames with equal beam and column stiffness under AISC and Eurocode semi-rigid connection stiffness range

Spec.	Connection Stiffness	Frame Condition	Fixed base	Hinged base
AISC (Secant Stiffness)	$2K_b < K_s < 20K_b$	Unbraced	31%	42%
		Braced	7%	9%
Eurocode (Initial Stiffness)	$0.5K_b < K_s < 8K_b$	Unbraced	53%	77%
	$0.5K_b < K_s < 25K_b$	Braced	12%	17%

Table 3 highlights the significant influence of the flexibility of bases and connections on the buckling capacity of frames. It indicates that reductions in buckling capacity are more pronounced in the case of unbraced frames, where base flexibility tends to further degrade the frame's buckling capacity appreciably. The reductions can be as large as 77% in some cases where connections are considered semi-rigid according to Eurocode provisions. Thus, simplifying moment connections as fully rigid in structural analysis models can lead to an overestimation of the load-carrying capacity of structures, while the flexibility of joints reduces the capacity substantially. This necessitates proper accounting for the stiffness of connections in analysis. In practice, one way to determine the actual stiffness of connections is by using the component method established in the Eurocode, where each component in a connection, such as bolts, framing angles, and end plates, is modelled as a linear spring with stiffness k_i, as depicted in Figure 18. The overall stiffness of the connection is then the collective stiffnesses of all the constituent components, calculated as follows: [30]

$$S_j = \frac{Ez^2}{\mu \sum 1/k_i} \tag{31}$$

Where:

- k_i: is the stiffness coefficient for the basic joint component i.
- z: is the lever arm, to be determined as per Eurocode provisions.
- μ: is the ratio of the stiffness S_j to the initial stiffness $S_{j,ini}$, determined in accordance with Eurocode provisions. The initial stiffness is the S_j calculated from Equation (31) with $\mu = 1$.

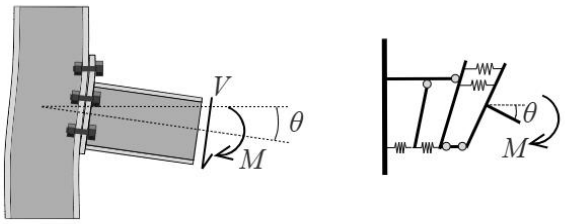

Fig. 18 Eurocode's component method for determining rotational stiffness of moment connection, modelling each component as a linear spring

The Eurocode provides a table of formulas for calculating the stiffness coefficients k_i of all components in a connection. The stiffness, S_j, can be substituted for K_s, and then used in the analytical or numerical frameworks devised in this paper. The Eurocode also specifies a detailed method for calculating column base stiffness, which can then be utilized in the four-spring frame model. This allows for all types of joints' flexibility to be properly accounted for in the stability analysis of steel structures.

5. Conclusion

This research studied the elastic stability of flexibly jointed structural steel frames. Two approaches were proposed: analytical and numerical. The analytical treatment utilized stability functions and proved superior in identifying the key parameters that directly affect stability. These parameters appear in the characteristic equation and are typically relative stiffness ratios of the beams, columns, and

connections that constitute the structure. The stiffness method, which is a numerical treatment of the subject, corroborated the analytical insights with high fidelity and with minimal deviation from theoretical predictions. The method utilized distinct spring elements to model connections' flexibilities and ensure rotational decoupling at the joints. The software "stableX" provides engineers with a practical, extensible, and effective tool for handling complex frame geometries with various loading and boundary conditions. Further, the application of the stiffness matrices in this paper extends to nonlinear incremental analysis, where the load-deformation response can be explored, and additional material nonlinearities could be considered. The paper also addressed the categorization criteria of current codes of practice in classifying steel connections as semi-rigid. The analysis highlighted that code-classified "semi-rigid" connections can cause reductions up to 77% in the stability of frames, underscoring the importance of incorporating joint stiffness in analysis. The reductions were particularly pronounced in unbraced frames, where hinged bases further amplified the reductions in buckling capacity. The dual analytical and numerical frameworks developed in this paper provide a valuable tool for engineers to assess the stability of flexibly jointed frames.

References

[1] Leonhard Euler, *A Method of Finding Curved Lines Enjoying the Property of Maximum or Minimum, or A Solution to the Isoperimetric Problem in the Broadest Sense*, Birkhäuser Basel, 1952. [Google Scholar] [Publisher Link]

[2] Marcello Pignataro, N. Rizzi, and A. Luongo, *Stability, Bifurcation, and Postcritical Behaviour of Elastic Structures*, Elsevier Science, 1991. [CrossRef] [Google Scholar] [Publisher Link]

[3] Stephen P. Timoshenko, and James M. Gere, *Theory of Elastic Stability*, Dover Publications, 2009. [CrossRef] [Google Scholar] [Publisher Link]

[4] Friedrich Bleich, Lyle B. Ramsey, and H. Bleich, *Buckling Strength of Metal Structures*, McGraw-Hill, 1952. [Google Scholar]

[5] Michael Rex Horne, and Wilfred Merchant, *The Stability of Frames: A volume in The Commonwealth and International Library: Structures and Solid Body Mechanics Division*, Elsevier Science, 1965. [CrossRef] [Google Scholar] [Publisher Link]

[6] R.K. Livesly, and D.B. Chandler, *Stability Functions for Structural Frameworks*, Manchester University Press, 1956. [Google Scholar]

[7] J.S. Przemieniecki, Theory of Matrix Structural Analysis, Dover Publications, 2012. [Google Scholar] [Publisher Link]

[8] John H. Argyris, and Sydney Kelsey, *Energy Theorems and Structural Analysis*, 1st ed., Springer New York, NY, 1960. [CrossRef] [Google Scholar] [Publisher Link]

[9] James A. Stricklin, Walter E. Haisler, and Walter A. Von Riesemann, "Geometrically Nonlinear Structural Analysis by Direct Stiffness Method," *Journal of the Structural Division*, vol. 97, no. 9, pp. 2299-2314, 1971. [CrossRef] [Google Scholar] [Publisher Link]

[10] Harold C. Martin, "*Large Deflection and Stability Analysis by the Direct Stiffness Metho*d," NTRS - NASA Technical Reports Server, 1966. [Google Scholar] [Publisher Link]

[11] J.H. Argyris, "Matrix Analysis of Three-Dimensional Elastic Media - Small and Large Displacements," *AIAA Journal*, vol. 3, no. 1, pp. 45-51, 1965. [CrossRef] [Google Scholar] [Publisher Link]

[12] William McGuire, Richard H. Gallagher, and Ronald D. Ziemian, *Matrix Structural Analysis*, 2nd ed., Create Space Independent Publishing Platform, 2000. [Google Scholar] [Publisher Link]

[13] Specification for Structural Steel Buildings (ANSI/AISC 360-22), American Institute of Steel Construction, 2022. [Online]. Available: https://www.aisc.org/products/publication/standards/aisc-360/specification-for-structural-steel-buildings-ansiaisc-360-16-download2/

[14] Eurocode 3: Design of Steel Structures - Part 1-1: General Rules and Rules for Buildings (EN 1993-1-1), European Committee for Standardization (CEN), 2005. [Online]. Available: https://www.phd.eng.br/wp-content/uploads/2015/12/en.1993.1.1.2005.pdf

[15] Miklos Ivanyi, and Charalambos C. Baniotopoulos, *Semi-Rigid Joints in Structural Steelwork*, 1st ed., Springer Vienna, 2000. [CrossRef] [Google Scholar] [Publisher Link]

[16] Wai-Fah Chen, Norimitsu Kishi, and Masato Komuro, *Semi-Rigid Connections Handbook*, J. Ross Publishing, 2011. [Google Scholar] [Publisher Link]

[17] Venkatesh Patnana, A.Y. Vyavahare, and Laxmikant M. Gupta, "Moment-Rotation Response for Semi-rigid Connections," *Recent Advances in Structural Engineering: Select Proceedings of SEC 2016*, vol. 1, pp. 313-326, 2018. [CrossRef] [Google Scholar] [Publisher Link]

[18] Ahmed Ajel Ali, "Numerical Investigation of Semi-Rigid Beam-to-Column Bolted Angle Connection," *Pollack Periodicals*, vol. 20, no. 3, pp. 16-23, 2025. [CrossRef] [Google Scholar] [Publisher Link]

[19] Fattouh Shaker, Mahmoud El-boghdadi, and Doaa Moussa Ali Moussa, "Finite Element 3-D Modelling of Semi-Rigid Steel Beam-to-Column Connections with Top-and-Seat and Double Web Angles," *Engineering Research Journal*, vol. 184, no. 4, pp. 209-225, 2025. [CrossRef] [Google Scholar] [Publisher Link]

[20] Huseyin Kursat Celik, and Gokhan Sakar, "Semi-Rigid Connections in Steel Structures: State-of-the-Art Report on Modelling, Analysis and Design," *Steel and Composite Structures*, vol. 45, no. 1, pp. 1-21, 2022. [CrossRef] [Google Scholar] [Publisher Link]

[21] Wai-Fah Chen, and N. Kishi, "Semirigid Steel Beam-to-Column Connections: Data Base and Modeling," *Journal of Structural Engineering*, vol. 115, no. 1, pp. 105-119, 1989. [CrossRef] [Google Scholar] [Publisher Link]
[22] Eric M. Lui, and Wai Fah Chen, "Analysis and Behaviour of Flexibly-Jointed Frames," *Engineering Structures*, vol. 8, no. 2, pp. 107-118, 1986. [CrossRef] [Google Scholar] [Publisher Link]
[23] Wai Fah Chen, and Eric M. Lui, "Effects of Joint Flexibility on the Behavior of Steel Frames," *Computers and Structures*, vol. 26, no. 5, pp. 719-732, 1987. [CrossRef] [Google Scholar] [Publisher Link]
[24] C.H. Yu, and Nandivararm Elumalai Shanmugam, "Stability of Frames with Semirigid Joints," *Computers and Structures*, vol. 23, no. 5, pp. 639-648, 1986. [CrossRef] [Google Scholar] [Publisher Link]
[25] Yoshiaki Goto, and Wai Fah Chen, "On the Computer-Based Design Analysis for the Flexibly Jointed Frames," *Journal of Constructional Steel Research*, vol. 8, pp. 203-231, 1987. [CrossRef] [Google Scholar] [Publisher Link]
[26] Tien Dung Nguyen, and Quoc Anh Vu, "Analysis of Steel Frame with Semi-Rigid Connections and Constraints Using a Condensed Finite Element Formulation," *International Journal of GEOMATE*, vol. 25, no. 111, pp. 113-121, 2023. [CrossRef] [Google Scholar] [Publisher Link]
[27] Abd Nacer Touati Ihaddoudène, Messaoud Saidani, and Mohamed Chemrouk, "Mechanical Model for the Analysis of Steel Frames with Semi Rigid Joints," *Journal of Constructional Steel Research*, vol. 65, no. 3, pp. 631-640, 2009. [CrossRef] [Google Scholar] [Publisher Link]
[28] U.V. Dave, and G.M. Savaliya, "Analysis and Design of Semi-Rigid Steel Frames," *Structures Congress 2010*, pp. 3240-3251, 2010. [CrossRef] [Google Scholar] [Publisher Link]
[29] Zdeněk P. Bažantand, and Luigi Cedolin, *Stability of Structures: Elastic, Inelastic, Fracture and Damage Theories*, World Scientific Connect, 2010. [CrossRef] [Google Scholar] [Publisher Link]
[30] Eurocode 3: Design of Steel Structures - Part 1-8: Design of Joints (EN 1993-1-8), European Committee for Standardization (CEN), 2005. [Online]. Available: https://www.phd.eng.br/wp-content/uploads/2015/12/en.1993.1.8.2005-1.pdf
[31] numpy.linalg.eig - NumPy v2.4.dev0 Manual, NumPy, 2025. [Online]. Available: https://numpy.org/devdocs/reference/generated/numpy.linalg.eig.html
[32] Robert Millard Jones, *Buckling of Bars, Plates, and Shells*, Bull Ridge Publishing, 2006. [Google Scholar] [Publisher Link]
[33] Christian Mittelstedt, *Buckling of Beams, Plates and Shells*, 1st ed., Springer Berlin, Heidelberg, 2024. [CrossRef] [Google Scholar] [Publisher Link]

Appendix 1

The derivations of Equations (27) and (28), which were previously introduced in Section 4, are provided in this appendix. Referring to Figure 17, the governing buckling load equation for the four-spring model is derived by formulating moment equilibrium equations at joints 2, 3, and 4. Joint 2 corresponds to the column-to-base interface, joint 3 to the column-to-connection interface, and joint 4 to the beam-to-connection interface. The base spring moment at Joint 2 is given by:

$$M_{21} = K_{s1}\theta_2 \tag{A.1}$$

The column end moments are expressed as:

$$M_{23} = nK_c\theta_2 - oK_c\theta_3 \tag{A.2}$$

$$M_{32} = -oK_c\theta_2 + nK_c\theta_3 \tag{A.3}$$

The connection spring moments at joints 3 and 4 are:

$$M_{34} = -M_{43} = K_{s2}\theta_3 - K_{s2}\theta_4 \tag{A.4}$$

The beam end moment at joint 4 is:

$$M_{45} = 4K_b\theta_4 + 2K_b\theta_5 \tag{A.5}$$

Since an anti-symmetrical sway buckling mode is assumed, it follows that $\theta_4 = \theta_5$. Therefore, Equation (A.5) simplifies to:

$$M_{45} = 6K_b\theta_4 \tag{A.6}$$

Applying moment equilibrium at each joint:

$$\sum M_2 = 0 \quad \rightarrow \quad M_{21} + M_{23} = 0 \tag{A.7}$$

$$\sum M_3 = 0 \quad \rightarrow \quad M_{32} + M_{34} = 0 \tag{A.8}$$

$$\sum M_4 = 0 \quad \rightarrow \quad M_{43} + M_{45} = 0 \tag{A.9}$$

Using Equations (A.1) to (A.6), the equilibrium equations become:

$$\sum M_2 = 0 \rightarrow K_{s1}\theta_2 + nK_c\theta_2 - oK_c\theta_3 = 0 \tag{A.10}$$

$$\sum M_3 = 0 \rightarrow -oK_c\theta_2 + nK_c\theta_3 + K_{s2}\theta_3 - K_{s2}\theta_4 = 0 \tag{A.11}$$

$$\sum M_4 = 0 \rightarrow -K_{s2}\theta_3 + K_{s2}\theta_4 + 6K_b\theta_4 = 0 \tag{A.12}$$

Rewriting in matrix form:

$$\begin{bmatrix} K_{s1} + nK_c & -oK_c & 0 \\ -oK_c & nK_c + K_{s2} & -K_{s2} \\ 0 & -K_{s2} & K_{s2} + 6K_b \end{bmatrix} \begin{Bmatrix} \theta_2 \\ \theta_3 \\ \theta_4 \end{Bmatrix} = 0 \tag{A.13}$$

Since non-trivial solutions for θ_2, θ_3, and θ_4 exist only when the determinant of the coefficient matrix is zero. Expanding the determinant and simplifying yields the following equation, which is Equation (27):

$$6\beta + n(1 + 6\beta\alpha_1 + 6\alpha_2) + \alpha_1(n^2 - o^2)(1 + 6\alpha_2) = 0 \quad \text{(A.14)}$$

For braced frames, column end moment equations involve different stability functions, namely, s and c. Equations (A.2) and (A.3) become:

$$M_{23} = sK_c\theta_2 + csK_c\theta_3 \quad \text{(A.15)}$$

$$M_{32} = sK_c\theta_2 + csK_c\theta_3 \quad \text{(A.16)}$$

Due to the symmetrical buckling mode, $\theta_4 = -\theta_5$. Thus, Equation (A.5) simplifies to:

$$M_{45} = 2K_b\theta_4 \quad \text{(A.17)}$$

Reformulating the equilibrium Equations (A.10) to (A.12) for the braced case yields the matrix equation:

$$\begin{bmatrix} K_{s1} + sK_c & csK_c & 0 \\ csK_c & sK_c + K_{s2} & -K_{s2} \\ 0 & -K_{s2} & K_{s2} + 2K_b \end{bmatrix} \begin{Bmatrix} \theta_2 \\ \theta_3 \\ \theta_4 \end{Bmatrix} = 0 \quad \text{(A.18)}$$

Expanding the determinant and simplifying leads to the following characteristic equation, which is Equation (28):

$$2\beta + s(1 + 2\beta\alpha_1 + 2\alpha_2) + \alpha_1 s^2(1 - c^2)(1 + 2\alpha_2) = 0 \quad \text{(A.19)}$$